Organic & Biomolecular Chemistry

ROYAL SOCIETY OF CHEMISTRY

COMMUNICATION

View Article Online
View Journal | View Issue

Cite this: *Org. Biomol. Chem.*, 2021, **19**, 9619

Received 2nd September 2021,
Accepted 17th October 2021

DOI: 10.1039/d1ob01720a

rsc.li/obc

Hydrogen bonding interactions can decrease clar sextet character in acridone pigments†

Zhili Wen, Lucas José Karas and Judy I-Chia Wu *

Computed nucleus-independent chemical shifts (NICS), contour plots of isotropic magnetic shielding (IMS), and gauge-including magnetically induced current (GIMIC) plots suggest that polarization of the π-system of acridones may perturb the numbers and positions of Clar sextet rings. Decreasing numbers of Clar sextets are connected to experimental observations of a narrowing HOMO–LUMO gap and increased charge mobility in solid-state assemblies of quinacridone and epindolidione.

Acridone pigments like quinacridone (**1**) and epindolidione (**2**) (a structural isomer of indigo) (Fig. 1) are low-cost, air-stable, and have use as paints, cosmetics, and printing inks, but their potential application as components of organic field-effect transistors has received little attention until the last decade.[1–5] These compounds were intentionally avoided in the designs of organic electronics, as the amine and carbonyl groups were thought to disrupt π-conjugation. Yet many solid-state pigments, containing N–H and C–O groups, have been found to exhibit high charge mobilities, rivaling those of acenes.[3–6] In the solid state, **1** has a hole mobility comparable to that of pentacene (0.1 *vs.* 0.1 $cm^2 V^{-1} s^{-1}$)[3] and **2** displays a hole mobility higher than that of tetracene (1.5 *vs.* 0.1 $cm^2 V^{-1} s^{-1}$).[4] It was suggested that hydrogen bonding can increase acene character of the monomers (see Fig. 1, imminium-enolate resonance structures on right).

Many N–H and C=O containing chromophores display large bathochromic UV-vis absorption shifts going from dilute solution to the solid state.[5–7] Quinacridone is yellow in solution, but turns red to violet in the solid state.[8,9] Epindolidione is blue in solution, and turns yellowish to orange in the solid state.[4] When dissolved in sulfuric acid, the doubly protonated quinacridone displays a narrower HOMO–LUMO gap than the neutral parent, showing a UV-vis spectrum similar to that of pentance.[5] These changes suggest that polarization of the π-system through hydrogen bonding, can reduce the HOMO–LUMO gaps of acridone pigments giving rise to increased charge mobility.[5] Hydrogen bonding interactions were found to improve the electronic properties of other conjugated organic systems[10,11] and donor–acceptor pairs.[12–14]

Here, we relate the known effects of enhanced charge mobility in hydrogen-bonded acridones to decreased aromaticity of the π-system.[15,16] First called the "aromatic sextet" in 1925,[17] and then proposed by Clar to follow a selective placement in polycyclic systems,[18] the "Clar sextet" describes a fully benzenoid ring where all π-electrons of a six membered ring belong to a single sextet. As shown in Fig. 1, **1** has three Clar sextets, and **2** has two, but polarization of the N–H and C=O sites enhance the contribution of "acene-like" resonance forms which can have only one Clar sextet.[19–21] In this way, hydrogen bonding self-assembly can reduce Clar sextet ratio of the acridone π-system, and the drop in Clar aromaticity can be related to a decreased HOMO–LUMO gap.[15,22,23] Isomers of closed-shell polyaromatic hydrocarbons (PAH) with fewer numbers of Clar sextets typically have lower ionization potentials, light

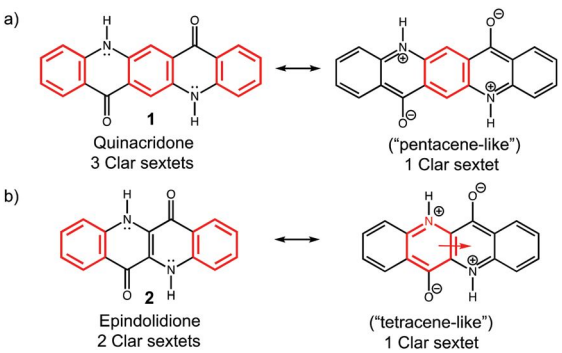

Fig. 1 (a) Quinacridone, (b) epindolidione, and their imminium-enolate resonance forms. Clar sextets are drawn in red. A red arrow across two rings indicates equivalent Clar structures.

Department of Chemistry, University of Houston, Houston, Texas 77204, USA. E-mail: jiwu@central.uh.edu

†Electronic supplementary information (ESI) available: Computed IMS plots, GIMIC plots, and NICS(1)$_{zz}$ values of 2-hydroxypyridine, 2-pyridone, 3, 3-pro, 3-taut, chrysene, and hydrogen-bonded trimers of **1–3**. Optimized Cartesian coordinates for all structures. See DOI: 10.1039/d1ob01720a

absorption shifted towards the visible region, and a smaller HOMO–LUMO separation.[24–30] We previously reported that formally non-aromatic organic dyes, like diketopyrrolopyrrole, naphthodipyrrolidone, indigo, and isoindigo, can show increased antiaromaticity upon hydrogen bonding.[31] The effects of intermolecular hydrogen bonding on aromaticity also can be seen in contrasting examples of the 2-pyridone dimer (aromaticity gain upon hydrogen bonding) and the 2-hydroxypyridine dimer (aromaticity loss upon hydrogen bonding) (see also supplementary data in the, ESI†).[32]

In this work, the Clar sextet patterns of **1** and **2** are compared to those of a doubly protonated form (**-prot**) and an acene-like tautomeric form (**-taut**), to model the highly polarized π-system of the monomers in the solid state. Fig. 1 shows, for each structure, the most representative resonance form with the largest number of Clar sextet(s).[18,33–35] Crystal structures of the α, β, and γ polymorphs of quinacridone[36–39] have C═O bond distances (*α*: 1.373 Å, *β*: 1.266 Å, *γ*: 1.299 Å) longer than the typical carbonyl C═O length (*ca.* 1.23 Å), indicative of strong π-polarization of the monomers in the solid state. Comparing this data to the computed C═O lengths for **1** (1.227 Å), **1-prot** (1.321 Å), and **1-taut** (1.352 Å) suggests that the π-systems of self-assembled quinacridone monomers may be appropriately modeled by the π-systems of **1-prot** and **1-taut**.

All geometries were optimized at B3LYP-D3/6-311+G(d,p)[40,41] with constrained C_{2h} symmetry for **1**, **2**, **1-prot**, **2-prot**, **1-taut**, and **2-taut** employing the Gaussian16 program.[42] Nucleus independent chemical shifts (NICS) computed at the PW91PW91/IGLOIII[43,44] level quantified aromaticity of the individual rings. NICS$(1)_{zz}$ values were computed at 1 Å above the ring centers and include only shielding tensor components from the out-of-plane "*zz*" direction.[45–48] Clar sextets are identified by a more negative NICS$(1)_{zz}$ in a ring compared to all of its neighboring rings. Isotropic magnetic shielding (IMS) plots were computed at the same level at 1 Å above the molecular plane using regular grids of points with an interval of 0.1 Å.[49] These plots were previously shown by Lampkin, Karadakov, and VanVeller to provide feature-rich descriptions of aromaticity and Clar sextet features in PAHs.[49] Gauge-including magnetically induced current (GIMIC) plots computed at B3LYP-D3/6-311+G(d,p) provided a visualization of the numbers and positions of Clar sextet(s).[50] Diatropic ring currents are indicated by intensified clockwise currents at the locations of the Clar sextets.[26] The computed IMS and GIMIC plots include magnetic shielding contributions from both the σ and π framework, and therefore cannot be compared directly to the computed NICS$(1)_{zz}$ results. Nevertheless, these plots provide qualitative information about the locations of the Clar sextets. Time-dependent (TD) density functional theory[51] computations were performed at TD-ωB97X-D/6-311+G(d,p)[52] to estimate the HOMO and LUMO levels of each model system. HOMO–LUMO gaps were derived by the HOMO to LUMO excitation energies.[53]

Fig. 2 compares the computed NICS$(1)_{zz}$ values of **1** and **2**, to their **-prot** and **-taut** forms, and acene reference. Based on computed NICS$(1)_{zz}$, **1** has three Clar sextets, each separated by a 4-pyridone spacer (note small negative NICS$(1)_{zz}$ values in the pyridone rings). The tautomer, **1-taut**, can have only one Clar sextet. The doubly protonated form, **1-prot**, represents an intermediate situation between the two, in which the NICS patterns identify three Clar sextets, but the "spacer" 4-pyridone rings have now gained significant aromatic character, suggesting that the electronic structure of the system is tending towards that of **1-taut**. Note that the NICS patterns of the individual rings of **1-taut** follow that of pentacene.

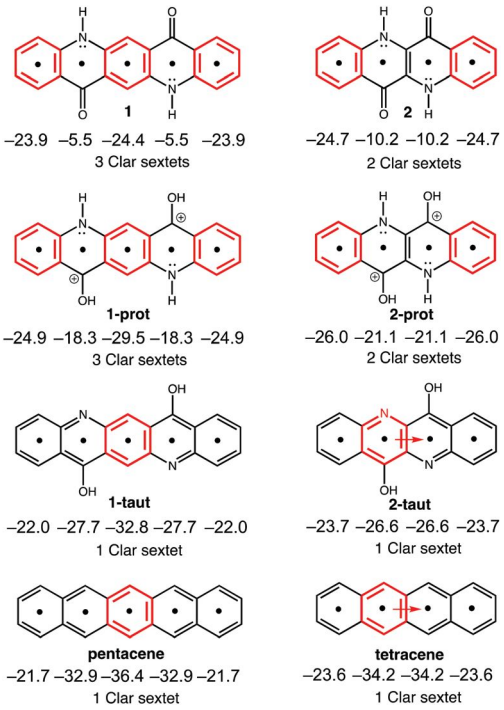

Fig. 2 Computed NICS$(1)_{zz}$ values for **1**, **1-prot**, and **1-taut**, compared to pentacene, and for **2**, **2-prot**, and **2-taut**, compared to tetracene. Clar sextets are drawn in red. A red arrow across two rings indicates equivalent Clar structures.

Like **1**, computed NICS$(1)_{zz}$ for **2**, **2-prot**, and **2-taut**, show increased diatropicity of the pyridone rings as the π-system becomes more polarized. NICS patterns of the individual rings of **2-taut** resemble those of tetracene, indicating one Clar sextet. In **2-taut** and in tetracene, the two central rings are equivalent Clar structures (indicated by a red arrow in Fig. 2) like that in naphthalene (*cf.* data for iso-epindolidione in the ESI,† where polarization of the π-system *increases* the number of Clar sextet rings). Remarkably, hydrogen bonding can reduce aromaticity in **1** and **2** by lowering the numbers of Clar sextets in the π-system. Consistent with experimental findings, the computed HOMO–LUMO gaps (Table 1) of both **1**, 3.23 eV (*cf.* 2.95 eV for a hydrogen-bonded trimer) and **2**, 3.52 eV (*cf.* 3.30 eV for a hydrogen-bonded trimer) become narrower upon hydrogen bonding at the N–H and C═O sites. Kinked systems like the iso-epindolidione (analogous to chrysene) show the opposite effect (*i.e.*, hydrogen bonding reduces the number of Clar sextets in the π-system. See data in the SI).

Table 1 Computed HOMO–LUMO gaps (in eV) for the monomer, hydrogen-bonded trimer, doubly protonated form, and tautomeric form of **1** and **2**

Cmpd.	Monomer	H-bonded trimer	Doubly protonated	Tautomer
1	3.23	2.95	2.50	2.44
2	3.52	3.30	2.84	3.03

Plots of isotropic magnetic shielding (IMS) (Fig. 3) were computed to visualize the Clar sextet patterns of **1**, **2** and their π-polarized analogs. The IMS plot of **1** shows three particularly shielded regions (>+12 ppm) at the positions of the arene rings, indicative of three Clar sextets. In **1-prot**, the central ring becomes even more shielded (see dark purple region, >+15 ppm), suggesting enhanced aromaticity, and the shielded areas of the terminal arene rings move towards the pyridone rings. In **1-taut**, the central ring is the most strongly shielded region (note cyclic dark purple region, indicating a Clar sextet, >+15 ppm), followed by the pyridone rings, and then the terminal arene rings (*cf.* IMS plot for pentacene). IMS plots for **2**, **2-prot**, and **2-taut**, show the same trends, suggesting a migration of the Clar sextets from the outer rings to the central rings (*cf.* IMS plot for tetracene).

Details of the induced ring currents of **1**, **2**, and their π-polarized analogs are shown in Fig. 4 by the gauge-including magnetically induced current (GIMIC) plots. **1** displays three localized diatropic ring currents, located at the positions of the arene rings. A weakly diatropic current encompasses the periphery of the five fused rings. **1-prot** shows a pronounced macrocyclic diatropic ring current around the periphery of the molecule which intensifies at the central ring and terminal rings. Note that only the central ring shows a complete localized diatropic ring current, while the terminal rings show a breached local ring current. In **1-taut**, the macrocyclic diatropic current becomes dominant, and is strongest at the central ring and weakest at the terminal rings. These features agree with the findings of NICS and IMS, showing a reduced Clar sextet ratio going from **1** (three Clar sextets), **1-prot**, to **1-taut** (one Clar sextet). GIMIC plots for **2**, **2-prot**, and **2-taut**, also shown an increasingly delocalized diatropic ring current. In **2**, there are two localized diatropic ring currents, located at the positions of the arene rings, indicating the presence of two Clar sextets. But as the π-system becomes increasingly polarized, a macrocyclic diatropic ring current dominates, and the GIMIC plots of **2-prot** and **2-taut**, become more tetracene-like.

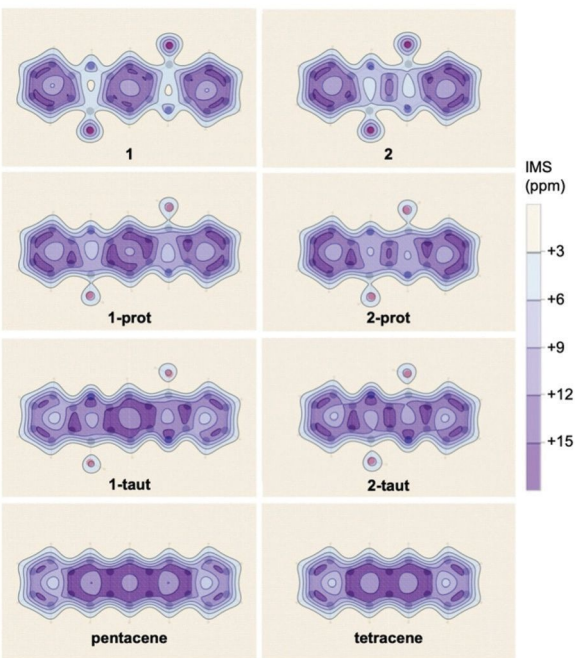

Fig. 3 Computed IMS plots for **1**, **1-prot**, and **1-taut**, compared to pentacene, and for **2**, **2-prot**, and **2-taut**, compared to tetracene.

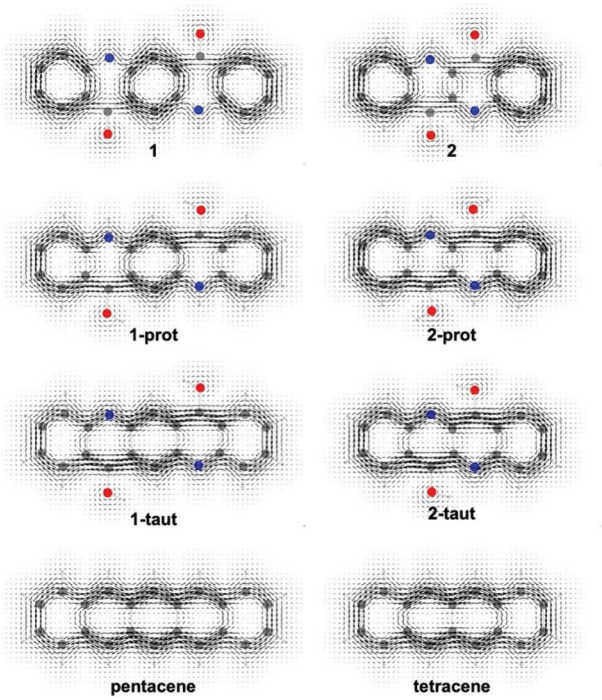

Fig. 4 Computed GIMIC plots for **1**, **1-prot**, and **1-taut**, compared to pentacene, and for **2**, **2-prot**, and **2-taut**, compared to tetracene.

Conclusions

Hydrogen bonding interactions can play an important role in the molecular design of organic semiconductors. Besides controlling solid state structure, it is helpful to recognize that hydrogen bonding interactions also can perturb the aromatic character of conjugated organic molecules, having relevant effects for their electronic properties. Here, we show that reducing the ratios of Clar rings can be considered as a design strategy to enhance charge transport property in popular organic dyes.

Conflicts of interest

The authors declare no competing financial interest.

Acknowledgements

We thank the National Science Foundation (CHE-1751370) and the Sloan Research Foundation (FG-2020-12811) for support. We also acknowledge use of the Sabine cluster and support from the Research Computing Data Core at the University of Houston.

Notes and references

1 M. Gsänger, D. Bialas, L. Huang, M. Stolte and F. Würthner, *Adv. Mater.*, 2016, **28**, 3615–3645.
2 H. Yanagisawa, J. Mizuguchi, S. Aramaki and Y. Sakai, *Jpn. J. Appl. Phys.*, 2008, **47**, 4728–4731.
3 E. D. Głowacki, L. Leonat, M. Irimia-Vladu, R. Schwodiauer, M. Ullah, H. Sitter, H. Bauer and S. Sariciftci, *Appl. Phys. Lett.*, 2012, **101**, 023305.
4 E. D. Głowacki, G. Romanazzi, C. Yumusak, H. Coskun, U. Monkowius, G. Voss, M. Burian, R. T. Lechner, N. Demitri, G. J. Redhammer, N. Sünger, G. P. Suranna and S. Sariciftci, *Adv. Funct. Mater.*, 2015, **25**, 776–787.
5 E. D. Głowacki, M. Irimia-Vladu, M. Kaltenbrunner, J. Gsiorowski, M. S. White, U. Monkowius, G. Romanazzi, G. P. Suranna, P. Mastrorilli, T. Sekitani, S. Bauer, T. Someya, L. Torsi and N. S. Sariciftci, *Adv. Mater.*, 2013, **25**, 1563–1569.
6 J. Weinstein and G. M. Wyman, *J. Am. Chem. Soc.*, 1956, **78**, 2387–2390.
7 E. D. Głowacki, G. Voss, L. Leonat, M. Irimia-Vladu, S. Bauer and N. S. Sariciftci, *Isr. J. Chem.*, 2012, **52**, 540–551.
8 J. Mizuguchi and T. Senju, *J. Phys. Chem. B*, 2006, **110**, 19154–19161.
9 S. S. Labana and L. L. Labana, *Chem. Rev.*, 1967, **67**, 1–18.
10 J. H. Oh, W.-Y. Lee, T. Noe, W.-C. Chen, M. Könemann and Z. Bao, *J. Am. Chem. Soc.*, 2011, **133**, 4204–4207.
11 H. Zhang, K. Liu, K.-Y. Wu, Y.-M. Chen, R. Deng, X. Li, H. Jin, S. Li, S. C. Chuang, C.-L. Wang and Y. Zhu, *J. Phys. Chem. C*, 2018, **122**, 5888–5895.
12 H. T. Black, N. Yee, Y. Zems and D. F. Perepichka, *Chem. – Eur. J.*, 2016, **22**, 17251–17261.
13 C.-H. Liu, M. R. Niazi and D. F. Perepichka, *Angew. Chem., Int. Ed.*, 2019, **58**, 17312–17321.
14 N. Yee, A. Dadvand and D. F. Perepichka, *Mater. Chem. Front.*, 2020, **4**, 3669–3677.
15 W. Chen, H. Li, J. R. Widawsky, C. Appayee, L. Venkataraman and R. Breslow, *J. Am. Chem. Soc.*, 2014, **136**, 918–920.
16 T. Stuyver, T. Zeng, Y. Tsuji, S. Fias, P. Geerings and F. D. Proft, *J. Phys. Chem. C*, 2018, **122**, 3194–3200.
17 J. W. Armit and R. Robinson, *J. Chem. Soc., Trans.*, 1925, **127**, 1604–1618.
18 E. Clar, *The Aromatic Sextet*, Wiley, London, 1972.
19 E. Steiner and P. W. Fowler, *Int. J. Quantum Chem.*, 1996, **60**, 609–616.
20 A. Soncini, P. W. Fowler and L. W. Jenneskenes, *Phys. Chem. Chem. Phys.*, 2004, **6**, 277–284.
21 P. v. R. Schleyer, M. Manoharan, H. Jiao and F. Stahl, *Org. Lett.*, 2001, **3**, 3643–3646.
22 C. Aumaitre and J.-F. Morin, *Chem. Rev.*, 2019, **19**, 1142–1154.
23 R. Gershoni-Poranne, A. P. Rahalkar and A. Stanger, *Phys. Chem. Chem. Phys.*, 2018, **20**, 14808–14817.
24 Y. Ruiz-Morales, *J. Phys. Chem. A*, 2002, **106**, 11283–11308.
25 Y. Ruiz-Morales, *J. Phys. Chem. A*, 2004, **108**, 10873–10896.
26 D. Moran, F. Stahl, H. F. Bettinger, H. F. Schaefer and P. v. R. Schleyer, *J. Am. Chem. Soc.*, 2003, **125**, 6746–6752.
27 A. T. Balaban and D. J. Klein, *J. Phys. Chem. C*, 2009, **113**, 19123–19133.
28 M. Solà, *Front. Chem.*, 2013, **1**, 22.
29 A. T. Balaban and D. J. Klein, *J. Phys. Chem. C*, 2009, **113**, 19123–19133.
30 J. C. S. Costa, R. M. Campos, L. M. S. S. Lima, M. A. V. R. da Silva and L. M. N. B. F. Santos, *J. Phys. Chem. A*, 2021, **125**, 3696–3709.
31 Z. Wen and J. I. Wu, *Chem. Commun.*, 2020, **56**, 2008–2011.
32 J. I. Wu, J. E. Jackson and P. v. R. Schleyer, *J. Am. Chem. Soc.*, 2014, **136**, 13526–13529.
33 E. Clar, *Polycyclic hydrocarbons*, Academic Press, London, 1964.
34 A. Misra, D. J. Klein and T. Morikawa, *J. Phys. Chem. A*, 2009, **113**, 1151–1158.
35 G. Portella, J. Poater and M. Solà, *J. Phys. Org. Chem.*, 2005, **18**, 785–791.
36 E. Paulus, F. J. J. Leusen and M. U. Schmidt, *CrystEngComm*, 2007, **9**, 131–143.
37 G. Lincke and H.-U. Finzel, *Cryst. Res. Technol.*, 1996, **31**, 441–452.
38 G. D. Potts, W. Jones, J. F. Bullock, S. J. Andrew and S. J. Maginn, *J. Chem. Soc., Chem. Commun.*, 1994, **22**, 2565–2566.
39 J. Mizuguchi, T. Sasaki and K. Tojo, *Z. Kristallogr. NCS*, 2002, **217**, 249–250.
40 S. Grimme, J. Antony, S. Ehrlich and H. Krieg, *J. Chem. Phys.*, 2010, **132**, 154104.
41 M. P. Andersson and P. Uvdal, *J. Phys. Chem. A*, 2005, **109**, 2937–2941.
42 M. J. Frisch, G. W. Trucks, H. B. Schlegel, G. E. Scuseria, M. A. Robb, J. R. Cheeseman, G. Scalmani, V. Barone, B. Mennucci, G. A. Petersson, H. Nakatsuji, M. Caricato, X. Li, H. P. Hratchian, A. F. Izmaylov, J. Bloino, G. Zheng, J. L. Sonnenberg, M. Hada, M. Ehara, K. Toyota, R. Fukuda, J. Hasegawa, M. Ishida, T. Nakajima, Y. Honda, O. Kitao, H. Nakai, T. Vreven, J. A. Montgomery Jr., J. E. Peralta, F. Ogliaro, M. Bearpark, J. J. Heyd, E. Brothers, K. N. Kudin, V. N. Staroverov, T. Keith, R. Kobayashi,

J. Normand, K. Raghavachari, A. Rendell, J. C. Burant, S. S. Iyengar, J. Tomasi, M. Cossi, N. Rega, J. M. Millam, M. Klene, J. E. Knox, J. B. Cross, V. Bakken, C. Adamo, J. Jaramillo, R. Gomperts, R. E. Stratmann, O. Yazyev, A. J. Austin, R. Cammi, C. Pomelli, J. W. Ochterski, R. L. Martin, K. Morokuma, V. G. Zakrzewski, G. A. Voth, P. Salvador, J. J. Dannenberg, S. Dapprich, A. D. Daniels, O. Farkas, J. B. Foresman, J. V. Ortiz, J. Cioslowski and D. J. Fox, *Gaussian 16; Revision C.01*, Gaussian, Inc. Wallingford, CT, 2016.

43 J. P. Perdew and Y. Wang, *Phys. Rev. B: Condens. Matter Mater. Phys.*, 1992, **45**, 13244–13249.

44 W. Kutzelnigg, *Isr. J. Chem.*, 1980, **19**, 193–200.

45 P. v. R. Schleyer, C. Maerker, A. Dransfeld, H. Jiao and N. J. R. v. E. Hommes, *J. Am. Chem. Soc.*, 1996, **118**, 6317–6318.

46 Z. Chen, C. S. Wannere, C. Corminboeuf, R. Puchta and P. v. R. Schleyer, *Chem. Rev.*, 2005, **105**, 3842–3888.

47 A. Stanger, *Eur. J. Org. Chem.*, 2020, 3120–3127.

48 R. Gershoni-Poranne and A. Stanger, in *Aromaticity: Modern Computational Methods and Applications*, ed. I. Fernandez, Elsevier, Amsterdam, 1st edn, 2021, ch. 4, pp. 99–154.

49 B. J. Lampkin, P. B. Karadokov and B. VanVeller, *Angew. Chem., Int. Ed.*, 2020, **59**, 19275–19281.

50 H. Fliegl, S. Taubert, O. Lehtonen and D. Sundholm, *Phys. Chem. Chem. Phys.*, 2011, **13**, 20500–20518.

51 E. Runge and E. K. U. Gross, *Phys. Rev. Lett.*, 1984, **52**, 997–1000.

52 A. D. Laurent and D. Jacquemin, *Int. J. Quantum Chem.*, 2013, **113**, 2019–2039.

53 J.-L. Bredas, *Mater. Horiz.*, 2014, **1**, 17–19.